



Contents lists available at SciVerse ScienceDirect

Tectonophysics

journal homepage: www.elsevier.com/locate/tecto

Seismic structure of the southeast Australian lithosphere from surface and body wave tomography

N. Rawlinson ^{a,*}, S. Fishwick ^b

^a Research School of Earth Sciences, Australian National University, Canberra, ACT 0200, Australia

^b Department of Geology, University of Leicester, Leicester LE1 7RH, UK

ARTICLE INFO

Article history:

Received 13 June 2011

Received in revised form 11 October 2011

Accepted 21 November 2011

Available online xxx

Keywords:

Seismic tomography

Surface waves

Body waves

Southeast Australia

Gondwana

ABSTRACT

Teleseismic arrival time residuals from the WOMBAT transportable seismic array experiment are inverted to construct a high-resolution 3-D P-wave velocity model of the upper mantle beneath southeast Australia. In order to address one of the principal limitations of teleseismic tomography – that long wavelength structure is filtered out when data from multiple arrays operating at different times are used – an initial model with lower spatial resolution, derived from surface tomography, is constructed to preserve the broad scale features that would otherwise be lost. Although the absolute velocities of the final model are not strongly constrained due to the assumption of radial V_p/V_s ratios and differences in regularisation, the relative variations appear robust across all scales. These reveal a wealth of features that can be related to the geology and tectonic history of the region, the most significant being (1) an easterly dipping velocity transition zone which involves a higher velocity Delamerian Orogen extending beneath the Western Subprovince of a lower velocity Lachlan Orogen; (2) a distinct region of low velocity in the upper mantle north of Melbourne, which can be associated with recent Quaternary hot-spot volcanism; (3) a gradual east-southeast decrease in velocity towards the coast, which is consistent with lithospheric stretching and thinning near a passive margin; and (4) a zone of high velocity north of Adelaide that may correspond to the presence of the Palaeoproterozoic Curnamona Province at depth. These results have important implications for the Palaeozoic evolution of the east margin of Gondwana, the subsequent break-up of Australia and Antarctica and opening of the Tasman Sea.

© 2011 Elsevier B.V. All rights reserved.

1. Introduction

Teleseismic traveltimes tomography, which exploits relative arrival time residuals from distant earthquakes to image crust and upper mantle structure beneath a seismic array, has been widely used in various parts of the world since the mid-1970s (e.g. Aki et al., 1977; Benz et al., 1992; Graeber et al., 2002; Oncescu et al., 1984; Rawlinson and Kennett, 2008; Saltzer and Humphreys, 1997). Reasons for its popularity as an imaging technique include (1) the relatively low cost of passive seismic deployments; (2) that local seismicity is not required, so it can be used almost anywhere; (3) that lateral resolution is a function of station spacing (and is limited only by the frequency of the impinging wavefront); and (4) the coherency of waveforms across the array, which enable high quality data to be extracted using cross-correlation type techniques (e.g. Chevrot, 2002; Rawlinson and Kennett, 2004; VanDecar and Crosson, 1990).

However, teleseismic traveltimes tomography also has a number of limitations, which have been widely recognised (Rawlinson et al.,

2010a). These include (1) that relative arrival time residuals contain information from outside the local model region; (2) that shallow structure beneath the array cannot be resolved due to a lack of crossing path coverage; and (3) that relative arrival times only constrain relative variations in wavespeed. The issue of shallow structure is an important one, particularly as many teleseismic arrays use stations spacings (> 30–40 km) that result in little or no crossing path coverage in the crust. Given that the crust is often highly heterogeneous, it is very likely that unwarranted structure will be mapped into the model region. One of the most common methods for addressing this problem is to include station terms in the inversion (e.g. Frederiksen et al., 1998; Graeber et al., 2002), which are designed to absorb the traveltimes residual contribution from the unresolved structure. However, the trade-off between station terms and velocity structure is difficult to resolve (Rawlinson and Kennett, 2008). An alternative approach is to use accurate *a priori* crustal models to account for shallow heterogeneity (e.g. Lei and Zhao, 2007; Martin et al., 2005; Waldhauser et al., 2002). Although preferable to the use of station terms, this approach only works if high quality prior information is available. Likewise, if data from local earthquakes or active source surveys are available, these can be simultaneously inverted with the teleseismic data to account for shallow structure (e.g. Rawlinson et al., 2010b).

* Corresponding author.

E-mail address: nicholas.rawlinson@anu.edu.au (N. Rawlinson).

The use of relative arrival times in teleseismic tomography is necessary in order to account for uncertainties in source origin time and broad scale heterogeneities along the path between source and the model region (which have an approximately uniform effect on the portion of the teleseismic wavefront that impinges on the receiver array). Apart from the limitation of relative velocity variations, the cost of removing the absolute reference frame from the data is that it becomes difficult to compare or combine data recorded at different times from adjacent arrays. This shortcoming is particularly relevant given the recent rise of transportable array experiments like USArray (e.g. Roth et al., 2008) in the US and WOMBAT (e.g. Rawlinson et al., 2011) in Australia. Rather than use relative arrival times in teleseismic tomography, one could use absolute arrival times and embed the local model into a lower resolution regional or global model, which is either provided *a priori* or is inverted for simultaneously (using, for example, data from global catalogues) with the teleseismic arrival times. This approach was used by Burdick et al. (2008) to build a high resolution model of the upper mantle beneath USArray, and has the twofold benefit of accounting for structure outside the model region and allowing data recorded by adjacent arrays to be properly combined. Although origin time uncertainty can be included as an unknown in the inversion, it will ultimately be a source of noise when absolute time is used, as will strong heterogeneity in the neighbourhood of the earthquake source.

Alternatively, information from surface waves can be used to provide improved vertical resolution, and to obtain further information on the absolute velocities. Simultaneous inversion of body wave and surface wave datasets has been applied at a global scale for a number of years (Antolik et al., 2003; Mégnin and Romanowicz, 2000). For regional studies West et al. (2004) developed a technique for the joint inversion of surface and body wave traveltimes. The method simply treats surface waves as horizontally propagating rays with deep sensitivity kernels, thus eliminating the problem of trying to combine datasets of different dimension. More recently, Obrebski et al. (2011) jointly invert surface-wave phase velocities and body wave traveltimes to obtain a high resolution 3-D model of the velocity structure beneath the western US.

In this study, we use complementary results from a continent-wide surface wave tomography model to account for the long wavelength structure that is filtered out when relative traveltime residuals recorded by multiple seismic arrays are simultaneously inverted. The technique is applied to data from the ongoing WOMBAT transportable array experiment in eastern Australia in order to significantly improve on previous imaging results that only exploited relative arrival time residual information.

2. Geological setting

The lithosphere beneath eastern Australia was formed during a protracted period of Palaeozoic orogeny that began in the Early Cambrian and terminated in the Middle Triassic (Glen, 2005). The initiation and continuity of this accretion was largely dictated by dynamic processes along the east Gondwana margin, which extended some 20,000 km along what was then the east margin of Precambrian Australia, through west Antarctica and into western Argentina. The new and reworked lithosphere that formed as a result of this activity, and now occupies the eastern third of the Australian continent, is commonly referred to as the Tasmanides or Tasman Orogen (Foster and Gray, 2000; Glen, 2005).

In southeast Australia, the Tasmanides comprise the Delamerian Orogen and the Lachlan Orogen (see Fig. 1) with the New England Orogen out-cropping along the coast northeast of the Sydney Basin. The Delamerian Orogen, which also includes the Adelaide Rift Complex, contains evidence of the break-up of Rodinia and subsequent development of the East Gondwana passive margin in the form of exposed late Neo-Proterozoic–early Cambrian rift-related sequences (Gibson et

al., 2011). Contractual orogenesis was initiated at approximately 514 Ma and continued to about 490 Ma (Foden et al., 2006), when a period of rapid uplift, cooling and extension commenced. Based on strain fabrics and spatial distribution of subduction-related igneous rocks, Foden et al. (2006) conclude that west dipping subduction against the eastern margin of Gondwana produced the Delamerian Orogeny, with slab roll back some 25 M.yr. later probably being responsible for its cessation.

South of mainland Australia, the Delamerian Orogen is thought to extend into western Tasmania, where it is commonly referred to as the Tyennan Orogen (Crawford et al., 2003; Reed et al., 2002). This connection is reinforced by several studies that have examined the age and geochemistry of various igneous rocks, related to both extensional and contractual tectonics, and found strong similarities. For example, Direen and Crawford (2003a, 2003b), have found paired suites of unusual ~580 Ma olivine rich mafic volcanics, together with rare ~515 Ma boninites in both western Victoria and the mainland Delamerian Orogen. Despite these similarities, there is still no consensus regarding the tectonic setting of the Tyennan and mainland Delamerian orogens; in the former case, Crawford and Berry (1992), Crawford et al. (2003) and Reed et al. (2002) argue for the obduction of an intra-oceanic arc as a result of continued easterly subduction outboard of Proterozoic continental crust. This, however, is at odds with a number of studies that favour westerly subduction during the Delamerian Orogen (e.g. Betts et al., 2002; Foden et al., 2006).

The Lachlan Orogen, which formed outboard of the Delamerian Orogen from 485 to 340 Ma (Kemp et al., 2009), represents the next orogenic phase in the progressive development of the Pacific margin of Gondwana. Its tectonic evolution is an area of particular controversy in Australian geology, probably due - at least in part - to the vast swath of younger cover sequences (see Fig. 1) which masks large tracts of the Palaeozoic basement. A number of plausible models have been put forward to explain the evolution of this region of lithosphere, including those that favour accretionary oceanic systems involving multiple coeval subduction zones (Foster and Gray, 2000; Spaggiari et al., 2003; Spaggiari et al., 2004) and those that argue for orogen-parallel strike-slip tectonics and the involvement of at least some pre-existing continental crust (Glen, 2005; Glen et al., 2009; Taylor and Cayley, 2000; VandenBerg, 1999; Willman et al., 2002). Another possibility is that fragments of continental crust, set adrift during the break-up of the supercontinent Rodinia, became embedded in the convergent accretionary system responsible for the formation of the Lachlan Orogen (Cayley et al., 2002; Doreen and Crawford, 2003b; Glen, 2005). One of the keys to solving this puzzle is to identify the extent to which the region is underlain by Palaeozoic lithosphere of oceanic origin, and Precambrian lithosphere of continental origin.

The Lachlan Orogen is commonly subdivided into three separate subprovinces (Foster and Gray, 2000), separated by major faults (see Fig. 1), which may represent lithospheric sutures. Due to a lack of extensive Palaeozoic outcrop, the locations of these faults are partly inferred from potential field data. As such, (Glen, 2005) infers the presence of a fourth subprovince - the southwestern subprovince - that essentially occupies the Melbourne and Bendigo zones in Fig. 1. Over the last half century, there have been numerous attempts to identify a southward continuation of the Lachlan Orogen in Tasmania (Leaman, 1994; Powell and Baillie, 1992; Talent and Banks, 1967), although to date a strong link remains elusive. In the last decade, it has been argued (Cayley, 2011; Cayley et al., 2002; Reed et al., 2002) that the Proterozoic core of Tasmania represents an exotic microcontinent which extends northwards and becomes the basement beneath the Melbourne Zone. In this case, eastern Tasmania may have affinities with the Tabberabbera Zone (Reed et al., 2002).

Historically, the boundary between the Lachlan and Delamerian orogens has been difficult to identify, with various possibilities put forward (e.g. Baillie, 1985; Foster and Gleadow, 1992; VandenBerg, 1978). More recently, with the help of high resolution potential

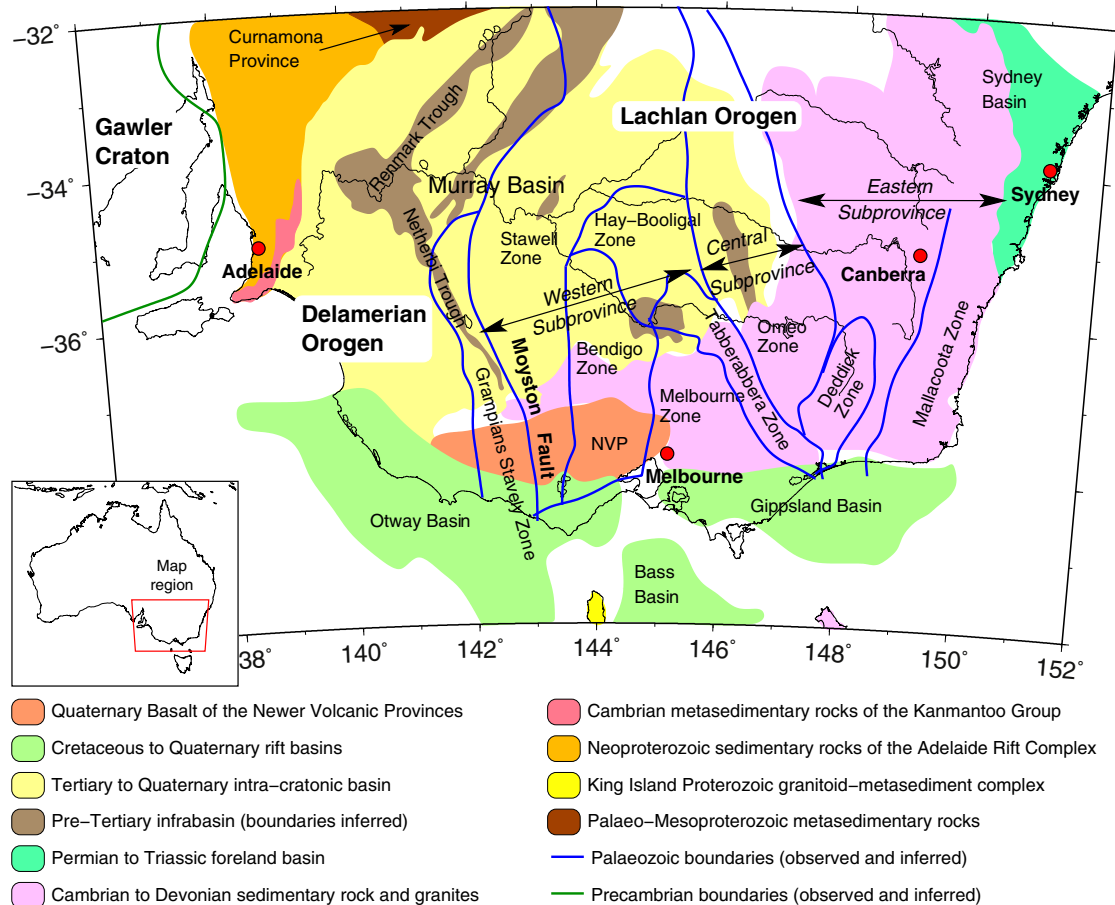


Fig. 1. Simplified geological map (based on Cayley et al., 2002, Foster and Gray, 2000 and Knight et al., 1995) showing observed and inferred Palaeozoic boundaries at the surface and approximate coverage of younger cover sequences.

field data and reflection seismic transects, the Moyston Fault (Fig. 1) has become the preferred location of the orogenic transition. Korsch et al. (2002) use deep reflection seismic data to identify an easterly dipping Moyston Fault at depth, and conclude that the Lachlan Orogen was thrust westwards over the upper part of the Delamerian Orogen as a result of westerly subduction towards the eastern margin of Gondwana.

Following the formation of the Tasmanides in eastern Australia, a number of subsequent tectonic events have conspired to obfuscate the geological, geochemical and geophysical signatures of the Palaeozoic terrane. The break-up of Australia and Antarctica and opening of the Tasman Sea between 80 and 90 Ma (Gaina et al., 1998), resulted in substantial lithospheric thinning near the present passive margin of southeast Australia. Between Victoria and Tasmania, the Mesozoic–Cainozoic Bass Basin represents a failed intracratonic rift basin (Gunn et al., 1997) that formed during the initial break-up of Australia and Antarctica. Substantial mafic underplating may be associated with the formation of passive margins, particularly if lithospheric scale detachment faults produce asymmetric margins (Lister et al., 1986; Lister et al., 1991).

Of the younger cover sequences which mask the southern Tasmanides, the most extensive is the vast intra-cratonic Murray Basin, which is composed of marine Tertiary sediments overlain by fluvial and aeolian Quaternary sediments (Knight et al., 1995). Further south, the economically important Otway, Bass and Gippsland basins were formed as a result of the break-up of Australia and Antarctica. In central and western Victoria, the Newer Volcanic Provinces (NVP) comprise an extensive cover of Quaternary basalt that originates from hot-spot volcanism (Price et al., 1997).

3. Data and method

Teleseismic data used in this study is sourced from the WOMBAT transportable seismic array project in southeast Australia (see Fig. 2). WOMBAT originated as a series of three consecutive array deployments – LF98, MB99, AF00 – in western Victoria and southeast South Australia between 1998 and 2000 which were collectively named MALT, and managed out of Monash University and Flinders University. From 2001, The Australian National University embarked on an intensive deployment programme aimed at achieving high density passive seismic coverage throughout eastern Australia, and used MALT as the springboard for the mainland deployments. To date, over 550 stations have been deployed during the course of 14 separate sub-array experiments. Station spacing in Tasmania is approximately 15 km, while on the mainland it is approximately 50 km. Vertical component short period (1 Hz natural frequency) sensors were used between 1998 and 2006, after which they were replaced by three-component sensors (also with a natural frequency of 1 Hz).

The main focus of research using WOMBAT data has so far been teleseismic tomography (Clifford et al., 2008; Graeber et al., 2002; Rawlinson and Kennett, 2008; Rawlinson et al., 2006a, 2006b; Rawlinson et al., 2011), where relative arrival time residuals are mapped as 3-D P-wave velocity perturbations beneath a set of simultaneously recording stations. In Tasmania, where broadside wide-angle reflection and refraction data are available (marine shot lines parallel to the coast recorded by land based stations), joint inversion of teleseismic and active source data has been carried out (Rawlinson and Urvoy, 2006; Rawlinson et al., 2010b). Ambient noise tomography, which in this case exploits Rayleigh wave energy generated by oceanic

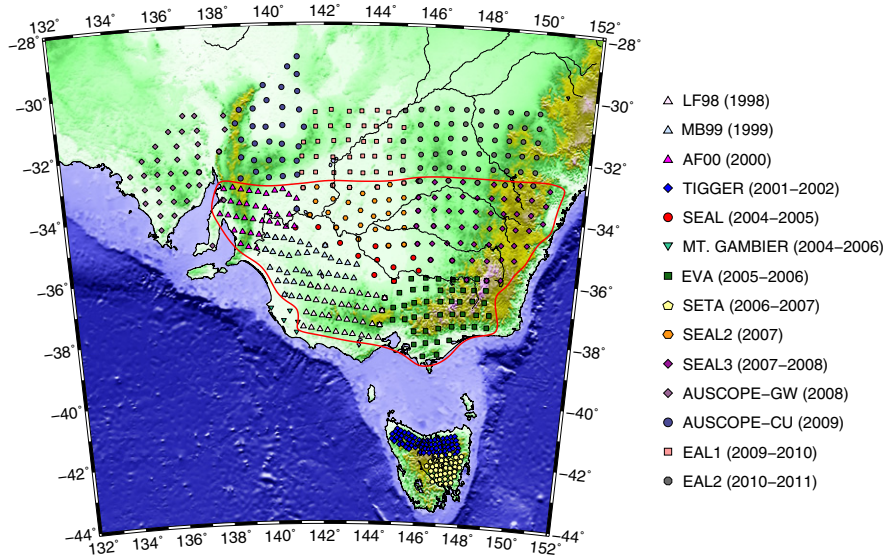


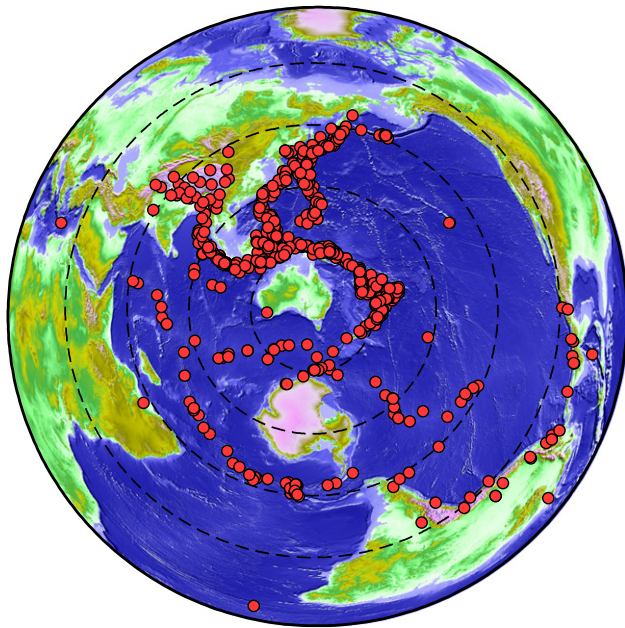
Fig. 2. Status of the WOMBAT transportable seismic array as of May 2011. The red line encloses the seven sub-arrays from which data were extracted for this study. Each separate deployment has its own network code (e.g. LF98). (For interpretation of the references to colour in this figure legend, the reader is referred to the web version of this article.)

microseisms, has been applied to the mainland data (Arroucau et al., 2010). Joint inversion of receiver functions and ambient noise dispersion curves from the SEAL3 array (see Fig. 2) has also been completed (Tkalcic et al., 2011).

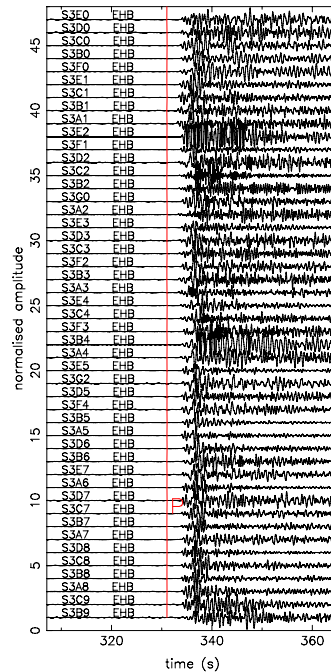
The teleseismic dataset used in the following work comes from seven mainland sub-arrays of the WOMBAT project (see Fig. 2) which together comprise a total of 282 stations. A variety of global body wave types are identified and picked using the adaptive stacking technique of Rawlinson and Kennett (2004), including direct P, PcP, ScP, PKiKP and PP. Fig. 3a shows the complete set of global events

from which data are extracted for this study. Most earthquakes exceed Mw 5.2 in size, although a number of deep focus events from subduction zones (e.g. Fiji) are less than Mw 5.0. Fig. 3b and c show examples of regional earthquakes recorded by the SEAL3 array following preliminary alignment using the ak135 global model (Kennett et al., 1995). In each case, the ak135 prediction (red line) appears to precede the onset of the P-wave, a phenomenon that is typical of the Australian region. Close examination of these plots shows that the traces do not perfectly align (up to 0.8 s offset), which indicates that lateral variations in wavespeed are present beneath the stations. For each source, the

(a) Teleseismic sources



(b) Fiji Islands, Mw=6.5



(c) Banda Sea, Mw=5.9

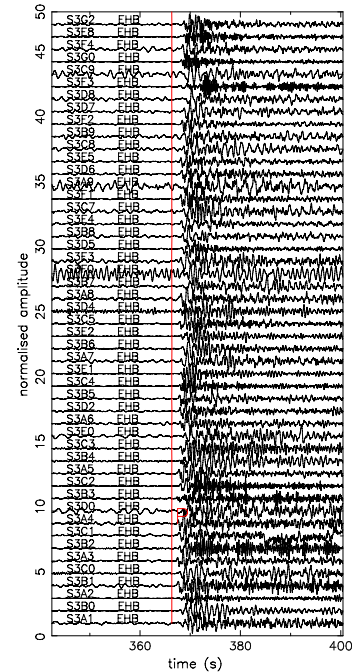


Fig. 3. (a) Distribution of teleseismic sources used in this study; (b) teleseismic P-waves from an earthquake that occurred in the Fiji Islands region on 15/01/2008, as recorded by the SEAL3 array; (c) teleseismic P-waves from an earthquake that occurred in the Banda Sea on 29/04/2008, as recorded by the SEAL3 array. Red lines in (b) and (c) denote ak135 predictions of the P-wave arrival. (For interpretation of the references to colour in this figure legend, the reader is referred to the web version of this article.)

mean is removed from the corresponding set of relative arrival times in order to create a complete set of relative arrival time residuals. Data binning is used to help mitigate the uneven distribution of earthquakes (Fig. 3a), which would otherwise result in strong smearing along rays that originate from regions of intense seismicity. Following this procedure, the total number of traveltime residuals available for tomography is 19,922. For further details on the data processing, refer to Rawlinson et al. (2011), which essentially uses the same set of arrival time residuals.

The principal difference between this work and the study of Rawlinson et al. (2011) is that surface wave data is here used to constrain the final 3-D model. Although joint inversion of surface and body wave data along the lines of the West et al. (2004) or Obrebski et al. (2011) study would be ideal for a transportable array like WOMBAT, the almost exclusive use of short period sensors means that surface waves in the period range required for complementary surface and body wave data coverage (30–150 s for Rayleigh waves) are simply not detected. Furthermore, WOMBAT is a 2-D array, not a linear array like that used by West et al. (2004), so the measurements of interstation surface wave traveltimes would have been much more difficult even if they were recorded. The alternative approach we use is to incorporate surface wave constraints via a surface wave tomography model of the Australian region constructed by Fishwick et al. (2008). In this study, a partitioned waveform inversion technique is applied to 2116 Rayleigh waveforms recorded by broadband instruments distributed throughout the Australian continent from earthquakes generated at the surrounding plate boundaries. The resultant 3-D shear wavespeed model of the upper mantle has a horizontal resolution in southeast Australia of about 250–300 km.

Due to the differences in coverage and resolution, it makes little sense to try and simultaneously invert the surface wave dataset and WOMBAT teleseismic arrival time residuals. Instead, we extract the region of the surface wave model that overlaps with the body wave coverage, and use it as an initial model in the inversion of the relative arrival time residuals. The minimum scale-length of the surface-wave model of around 250 km ideally complements the body wave data, which cannot resolve lateral structures that are greater in width than the aperture of the separate sub-arrays. As Fig. 2 shows, this generally varies between 250 and 500 km. Thus, the longer wavelength features that are effectively erased by converting body wave arrival times to relative arrival time residuals are re-inserted in the tomography in the form of a broad-scale heterogeneous starting model.

The availability of only P-wave arrival time residuals for this study – since teleseismic S-waves are very hard to detect on short period instruments – means that we need to combine P-wave data with an S-wave initial model. One option is to convert the S-wave model into a P-wave model by using prior knowledge of V_p/V_s ratios. Here, we simply assume $ak135$ V_p/V_s ratios due to a lack of more detailed information. Although regional traveltime tomography has been carried out using data recorded by some of the same stations used in the study of Fishwick et al. (2008), which have yielded both P-wave and S-wave velocity models (Kennett, 2003), the resolution in southeast Australia is poor, and not comparable with the surface wave tomography results. However, there is little evidence for significant differences in lateral velocity perturbations between the P- and S-wave models, so the assumption of laterally invariant V_p/V_s ratios appears reasonable at this scale. Nonetheless, we recognise that this is an important assumption, and acknowledge that it will affect the final result. In particular, the absolute velocity values that are recovered are likely to be less reliable. Compared to methods that simply add a regional 1-D model to the relative arrival time residual results to obtain absolute velocity (Allen et al., 2002; L ev eque and Masson, 1999), our approach is preferable because it takes into account lateral variations in wavespeed.

An iterative non-linear inversion method is used to map relative arrival time residuals as 3-D perturbations in wavespeed using the

surface wave model as a starting model. A grid based eikonal solver (Rawlinson and Sambridge, 2004) is used to solve the forward problem of predicting relative arrival times and a subspace inversion scheme (Kennett et al., 1988) is used to solve the inverse problem of adjusting model parameters to better satisfy data observations. Both damping and smoothing regularisation are applied in order to obtain a final model that suppresses the presence of poorly resolved structure while at the same time satisfying the data as well as possible. Station terms are also included as unknowns in the inversion in an attempt to minimise the mapping of unresolved crustal structure into the mantle model. While the inclusion of an accurate *a priori* crustal model would be preferable, no such model exists for southeast Australia. Rawlinson and Kennett (2008) perform numerical tests to examine the relative merits of station terms and *a priori* crustal models, and conclude that significant differences in the results only begin to occur above 70 km in depth.

4. Results

4.1. Synthetic tests

Before presenting the inversion results from the combined surface and body wave study, we first examine the spatial resolving power of the body wave data using synthetic checkerboard tests (e.g. Rawlinson et al., 2010a). Results for equivalent tests carried out with the surface wave data used to constrain the initial model can be found in Fishwick et al. (2008), which shows good resolution in southeast Australia, as reflected by a map of path coverage shown in Fig. 4. The goal of a synthetic test is to try and reconstruct a known model using the same source-receiver paths as the observational dataset. The forward problem (in this case the prediction of relative arrival time residuals) is solved in the presence of the synthetic model, using identical sources, receivers and phases as the actual dataset. This synthetic dataset then substitutes for the observed dataset and the inversion is initiated using the same initial parameters (initial model, damping, smoothing) as before. With a checkerboard test, the synthetic model consists of an alternating pattern of low and high velocities across all dimensions. It is often favoured in seismic tomography (e.g. Glahn and Granet, 1993; Graeber and Asch, 1999;

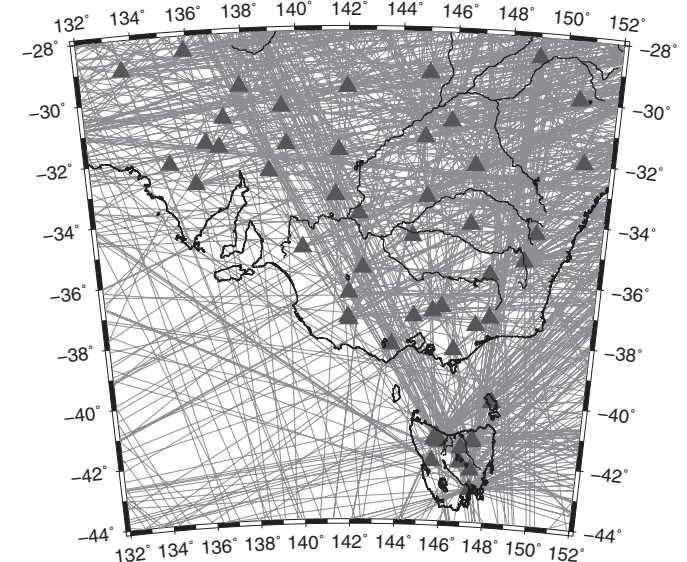


Fig. 4. Surface wave path coverage used to constrain the background velocity model that is used in the inversion of body wave arrival time residuals. Grey triangles denote recording stations used in the study of Fishwick et al. (2008).

Hearn and Clayton, 1986; Rawlinson and Urvoy, 2006; Rawlinson et al., 2011) because a continuous pattern makes interpretation relatively straight forward; however, it cannot be regarded as a comprehensive test of solution robustness (L  v  que et al., 1993).

Figs. 5–7 show the results of a synthetic checkerboard test carried out with the WOMBAT dataset. In order to better simulate observed data, Gaussian noise with a standard deviation of 50 ms has been added to the synthetic dataset. The input model is the synthetic checkerboard model, and the output model is the inversion result, which given an ideal dataset, would mimic the input model precisely. The long wavelength structure in all these plots is due to the presence of the broad scale-length surface-wave model which we use as an initial model. The reconstructed depth slices (Fig. 5) suggest that structure inboard of the coastline is quite well recovered, although some smearing is evident immediately inland of the coast. This is unsurprising given that the seismic arrays are all land-based. The E-W cross-sections (Fig. 6) indicate that structure is well resolved to a depth of 250–300 km, and in fact gross lateral variations in velocity to a depth of 50 km are also well constrained. However, given that crustal structure is likely to be complex, it is still necessary to include station correction terms in the inversion. The N-S slices clearly reveal the dimension in which smearing is most apparent. This occurs due to the fact that the earthquake source distribution is not uniform in azimuth (see Fig. 3a) – despite the application of source sub-binning – with the dominant region of seismicity occurring in an arc from the northwest to the northeast at angular distances ranging between 30 and 90  . As a result smearing is evident that has an approximately northerly dip angle of around 45  . Although this distortion of the checkerboard needs to be accounted for in the interpretation, the basic alternating pattern of anomalies is nonetheless recovered. Another observation that can be made about the synthetic tests is that amplitude is almost universally underestimated. This is a

common phenomena in reconstruction tests (Rawlinson et al., 2010a), and is due to the use of regularisation like damping and smoothing to promote the recovery of structure that is required by the data, and the suppression of anomalies that are poorly constrained.

4.2. WOMBAT model

Figs. 8–10 show a series of horizontal and vertical cross-sections through the final model produced by inversion of WOMBAT teleseismic data. In each case, the initial model based on surface wave data alone is shown, which helps distinguish the features that are recovered by the inversion of body wave traveltime residuals and those that are constrained by only the surface wave data. Six iterations of the tomographic scheme are used to reduce the RMS traveltime residuals from 286 ms to 137 ms, which corresponds to a variance reduction of 77%. If a laterally homogeneous initial model is used instead, the RMS traveltime residual drops from 244 ms to 143 ms, so clearly no shorter wavelength information is lost through the inclusion of surface wave constraints. The addition of body wave data has resulted in the presence of a rich array of features (Figs. 8–10) that the surface wave dataset is unable to resolve. However, these shorter wavelength structures would be difficult to interpret robustly in the absence of the underlying broadscale velocity variations supplied by the surface wave tomography. Therefore, this symbiotic process of combining surface and body wave information appears to result in a model that exhibits the best of both worlds. That said, it is worth recalling the assumptions and approximation made by the scheme which were outlined in the previous section, particularly the caveat regarding absolute velocities, which are not as well constrained as relative velocities.

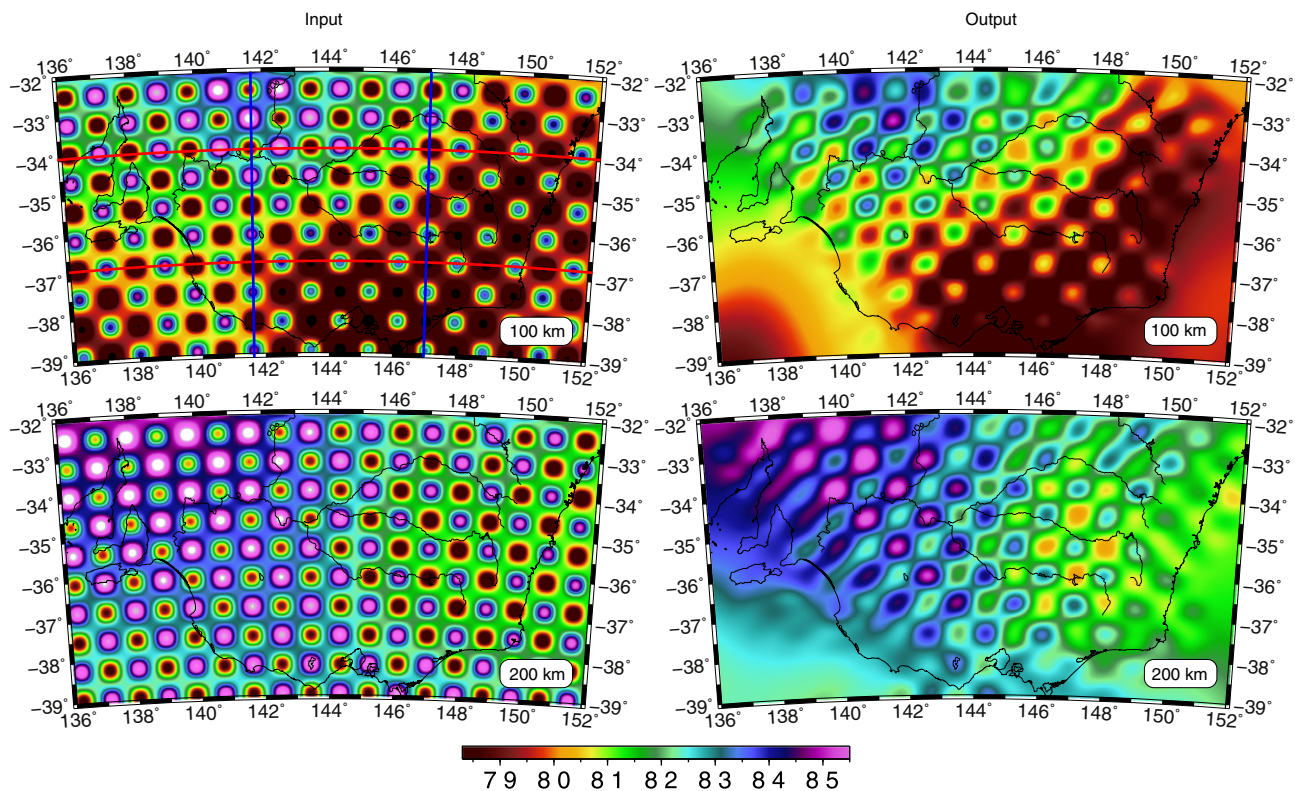


Fig. 5. Synthetic checkerboard resolution test results. The left column shows horizontal slices taken through the synthetic or input model at 100 km and 200 km depth. The right column shows the recovered pattern (or output) of anomalies. The long wavelength velocity variations present in the input and output models are due to the use of a laterally heterogeneous starting model. The red and blue horizontal and vertical lines in the top left plot indicate the location of E–W and N–S cross sections shown in Figs. 6 and 7 respectively. (For interpretation of the references to colour in this figure legend, the reader is referred to the web version of this article.)

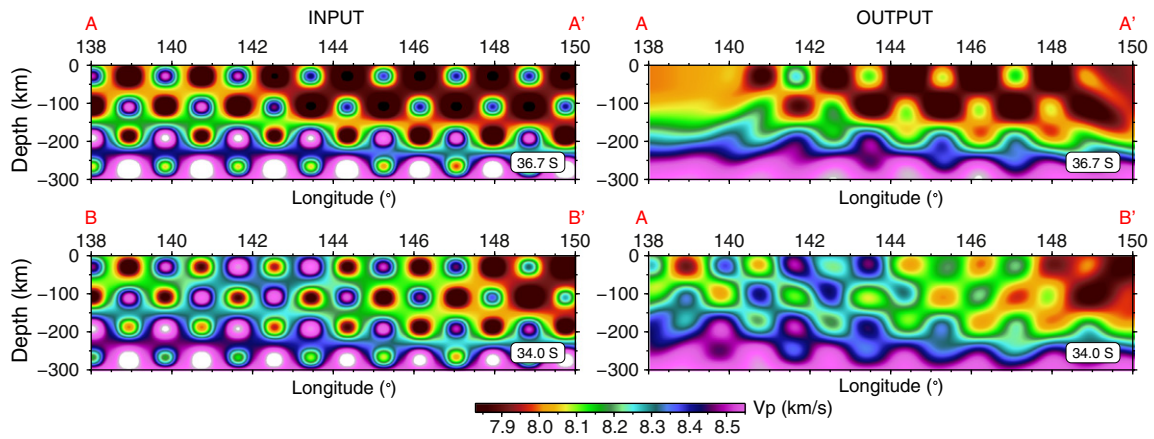


Fig. 6. E–W cross-sections through the input and output checkerboard models. See Fig. 5 for locations of the cross-sections.

A feature common to all vertical cross-sections (Figs. 9 and 10), which is also present in the checkerboard tests (Figs. 6 and 7), is that below around 120–150 km depth, the absolute velocity variations are dominantly in the vertical direction. According to the global reference model *ak135*, P-wavespeed varies by only 0.01 km/s between 35 and 120 km depth, but by 0.6 km/s between 120 and 310 km depth. At the shallower depths both the surface wave and body wave datasets introduce strong lateral variations, predominately due to the large contrasts in temperature between regions of varying lithospheric thickness. Towards the base of the model, while some lateral variability remains, the dominant control is the radial increase in velocities due to the larger effect of increasing pressure in comparison to smaller temperature variations within the convecting mantle.

The combined surface wave and body wave model (Figs. 8–10, right column) is generally well resolved in-board of the coast. Where body wave coverage is minimal, the solution model reverts to the surface wave model (e.g. in the southwest region of the 100 km depth slice in Fig. 8). Structural distortion due to streaking, which is caused by dominant raypath orientations, is most likely to occur in the N–S direction, according to the checkerboard tests (Fig. 7). Therefore, the slightly northerly dip of several anomalous structures in Fig. 10 (right column)

need to be viewed with caution. Both the surface and body wave dataset only poorly constrain crustal structure. Furthermore, unresolved crustal heterogeneity may map into uppermost mantle structures, so we tend to avoid interpreting velocity anomalies at depths above about 70 km (Rawlinson and Kennett, 2008).

5. Discussion

The new 3-D P-wave velocity model of southeast Australia, created by inverting relative arrival time residuals from the WOMBAT transportable array in the presence of an initial model obtained by regional surface wave tomography, reveals a variety of structures in the mantle that can be associated with the tectonic and geological evolution of the Australian plate from the Proterozoic to the Quaternary (see Fig. 11). The oldest outcrop that can be found within the bounds of the model region occurs in the southern Curnamona Province of South Australia (Fig. 1). Most prominent is the Willyama Supergroup, which is a Palaeoproterozoic belt of high-grade metasediments and meta-volcanics, and includes the Broken Hill, Olary and Eurioiwie blocks (Webster, 1996). The Curnamona Province was most likely part of a larger cratonic region that included the Gawler Craton (Fig. 1), but is now separated by Neo-Proterozoic

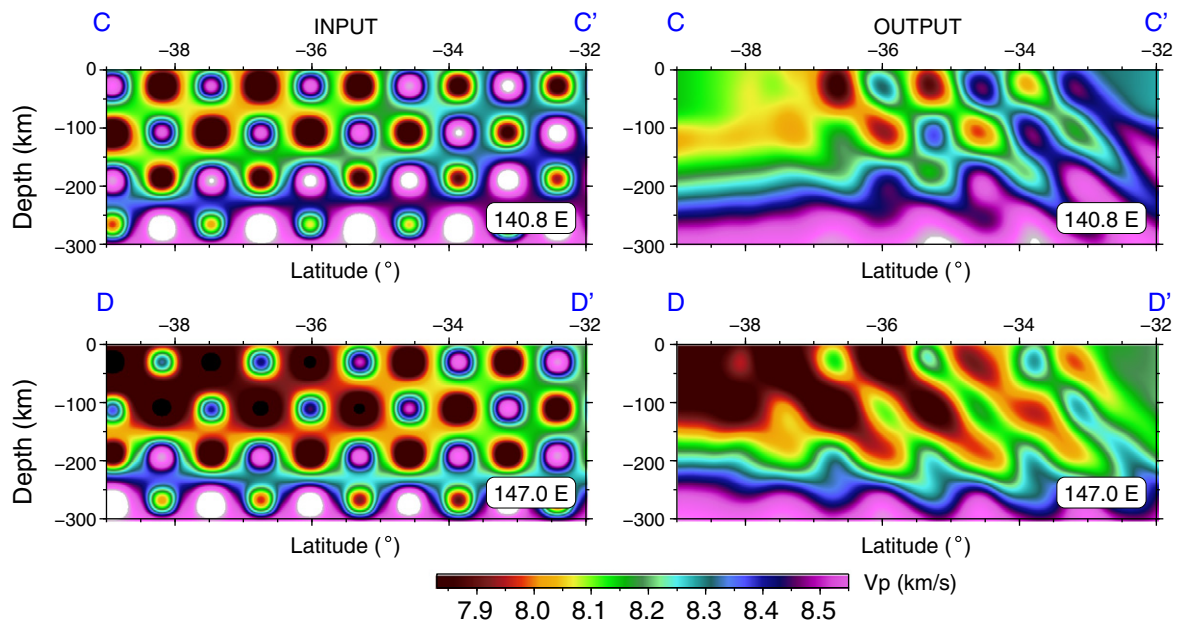


Fig. 7. N–S cross-sections through the input and output checkerboard models. See Fig. 5 for locations of the cross-sections.

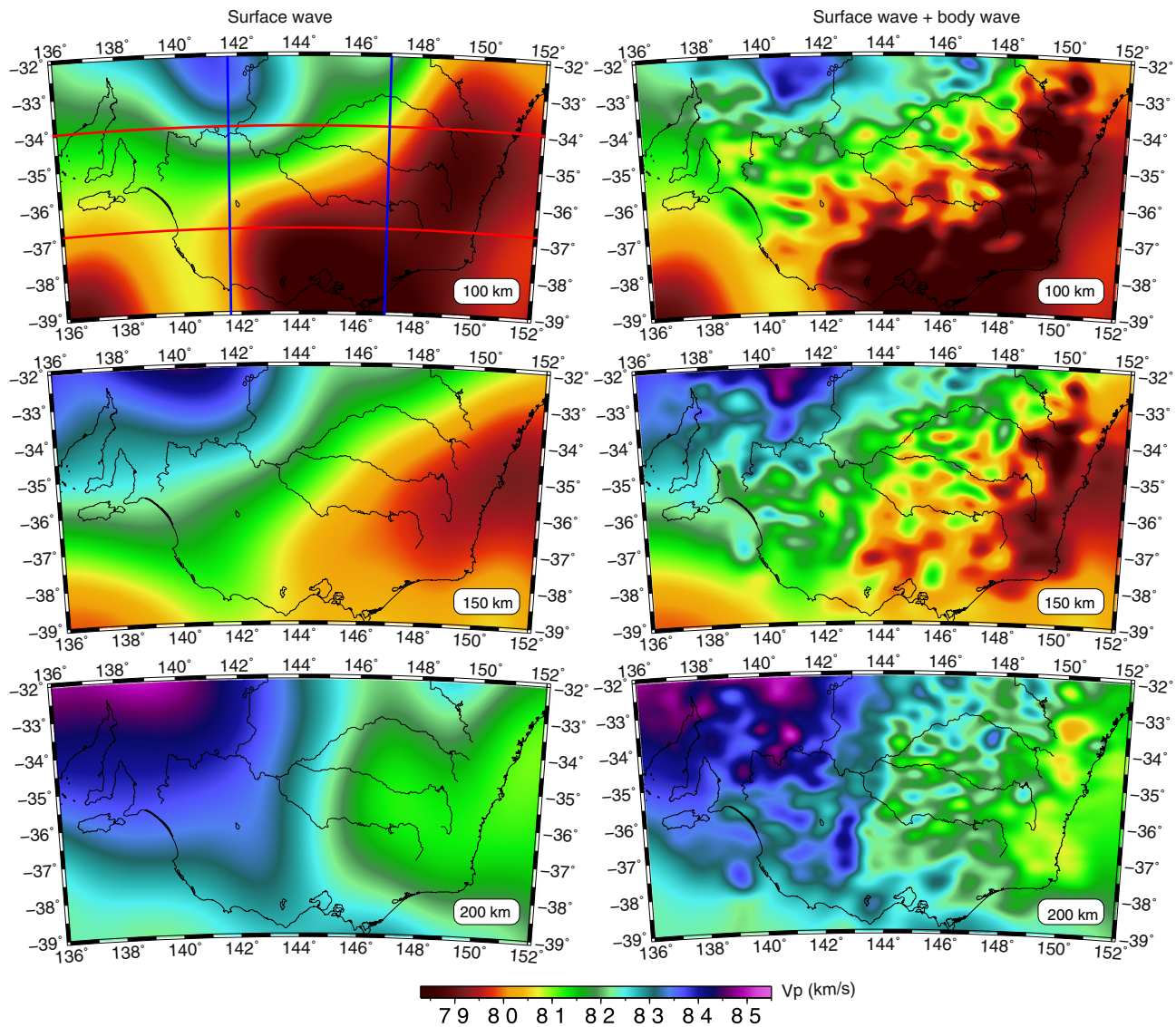


Fig. 8. Horizontal sections through the 3-D tomographic model constrained by surface waves only (left column), and by surface and body waves (right column). The red and blue horizontal and vertical lines in the top left plot indicate the location of E-W and N-S cross sections shown in Figs. 9 and 10 respectively. (For interpretation of the references to colour in this figure legend, the reader is referred to the web version of this article.)

sedimentary rocks of the Adelaide Rift Complex (Conor and Preiss, 2008). While the Curnamona Province was originally recognised to have properties typical of a Precambrian craton, subsequent studies have indicated that peripheral regions of the province were deformed and metamorphosed during the Delamerian Orogeny (Conor and Preiss, 2008). Hence, the term “Curnamona Craton” has largely given way to “Curnamona Province”.

A region of elevated velocity can be clearly observed in the north-west sector of the model (e.g. Fig. 11a), and is most likely related to the presence of the Curnamona Province. Previous tomography studies of the Australian continent (e.g. Debayle and Kennett, 2000; Fichtner et al., 2009; Fishwick et al., 2005; Simons et al., 1999; Yoshizawa and Kennett, 2004; Zielhuis and van der Hilst, 1996) show that cratons exhibit higher seismic velocities than surrounding regions of the lithospheric mantle, and likely penetrate deeper into the sublithospheric mantle. Hence, the high velocity anomaly that is observed to depths of at least 200 km is consistent with a piece of cratonic lithosphere. The fact that the region of elevated velocity is much more extensive than the Palaeo-Mesoproterozoic outcrop (cf. Fig. 1 and Fig. 11a,b) indicates that at least at lithospheric mantle

depths, the Curnamona Province extends for some distance south beneath the Murray Basin.

One of the main features of the model, as highlighted in Fig. 11a–c, is a strong west–east transition from higher to lower velocities that trends in the NNE direction. We regard this as a strong signature of the boundary between the Delamerian and Lachlan orogens at depth, and note that it has been considerably accentuated by the inclusion of body wave data, (cf. Fig. 8 left and right columns). This result suggests that a large chunk of the Delamerian Orogen underlies the Lachlan Orogen, and in fact that the boundary between the two terrains is east dipping at depth. This is consistent with the seismic reflection study of Korsch et al. (2002), which detects an east dipping reflector to a depth of about 15 km, that is inferred to be the Moyston Fault. The observed change in velocity between the Delamerian and Lachlan orogens is consistent with a change from Proterozoic mantle lithosphere of continental origin to Phanerozoic mantle lithosphere of oceanic origin. Expected changes in both composition (Cammarano et al., 2003; Griffin et al., 1998) and temperature (Faul and Jackson, 2005) between these two types of material support this view.

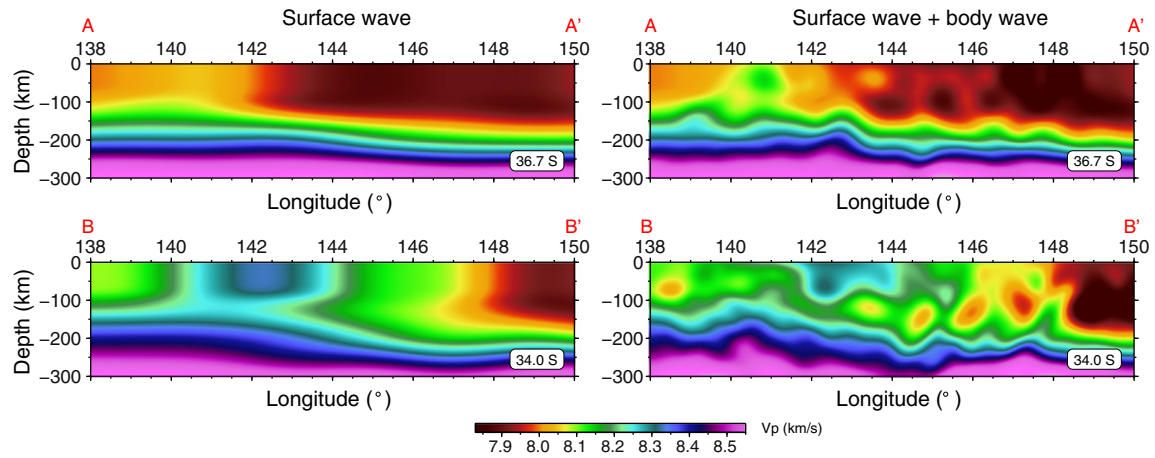


Fig. 9. E–W cross sections through the 3-D tomographic model constrained by surface waves only (left column), and by surface and body waves (right column). See Fig. 8 for locations of cross-sections.

The depths at which the Delamerian–Lachlan boundary is most clearly observed in the 3-D model, which is between 150 and 200 km, probably correspond to the very base of the lithosphere or perhaps even below. Surface wave tomography of the Australian region has previously shown that the lithosphere can be as thick as 250 km beneath Archean cratons in Western Australia (Fishwick et al., 2005; Simons et al., 2002). However, further east, particularly as we enter the Tasmanides, the lithosphere is likely to be much thinner. Fishwick et al. (2008) provide an estimate of lithospheric thickness beneath eastern Australia based on the depth extent of fast anomalies obtained from surface wave tomography. According to these results, the lithosphere may be as thick as 150–200 km beneath the Delamerian Orogen, but markedly thinner (~100 km) beneath the Lachlan Orogen, and thinning towards the coast to as little as 50 km. The dominant first-order E–SE decrease in velocity that can be seen in the 100 km depth slice (Fig. 8) is most likely due to a thinning of the lithosphere towards the passive margin. The consequence of these observations is that the velocity

contrast that we interpret as the Delamerian–Lachlan boundary may in fact represent a change from lithosphere in the west to sub-lithospheric mantle in the east. Alternatively, if it really is due to a velocity change within the mantle lithosphere, then it may be vertical smearing (see Fig. 7) that is responsible for its manifestation at such great depths.

One of the challenges in trying to interpret structure that was emplaced in the distant past from present day geophysical images is that subsequent deformation and alteration will overprint pre-existing features. Significant tectonic events that post-date the formation of the Tasmanides include the break-up of Australia and Antarctica and opening of the Tasman sea. Both these events resulted in substantial thinning of the lithosphere towards the passive margin. The lower velocities observed in the southeast region of the 100 km depth slice (Fig. 8, top), may be a result of elevated temperatures associated with the rifting and the presence of a thinner lithosphere. The strong low velocity signal observed in the surface wave model may also be enhanced by the thicker crust beneath the Great Dividing Range, which traverses the east coast of

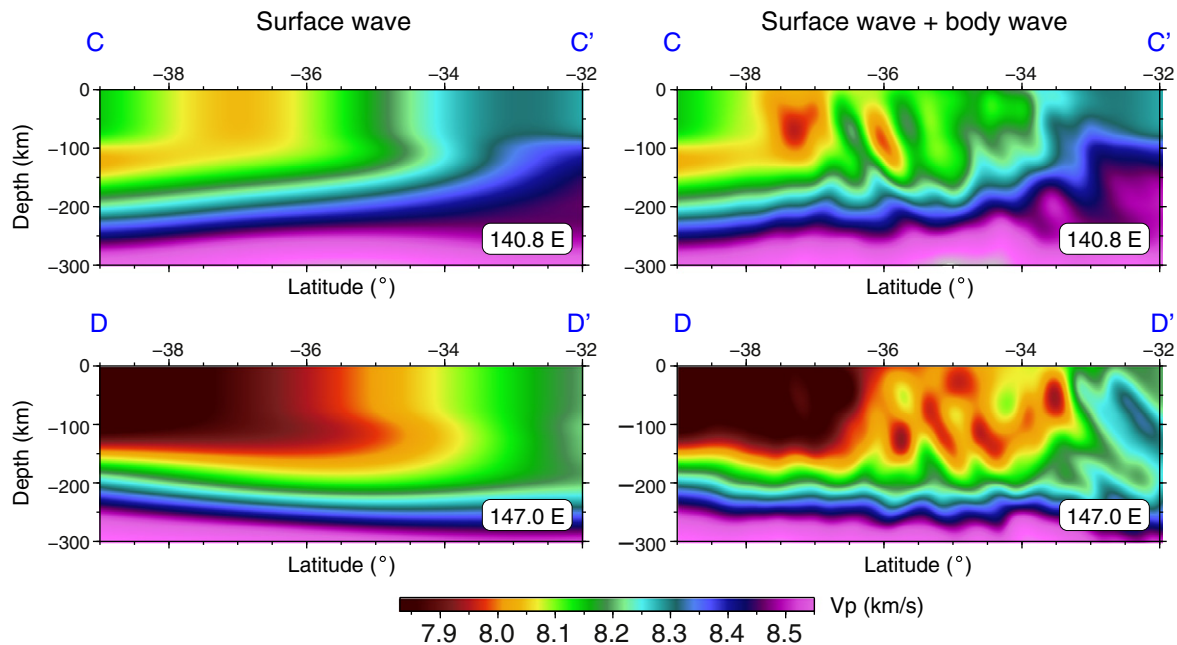


Fig. 10. N–S cross sections through the 3-D tomographic model constrained by surface waves only (left column), and by surface and body waves (right column). See Fig. 8 for locations of cross-sections.

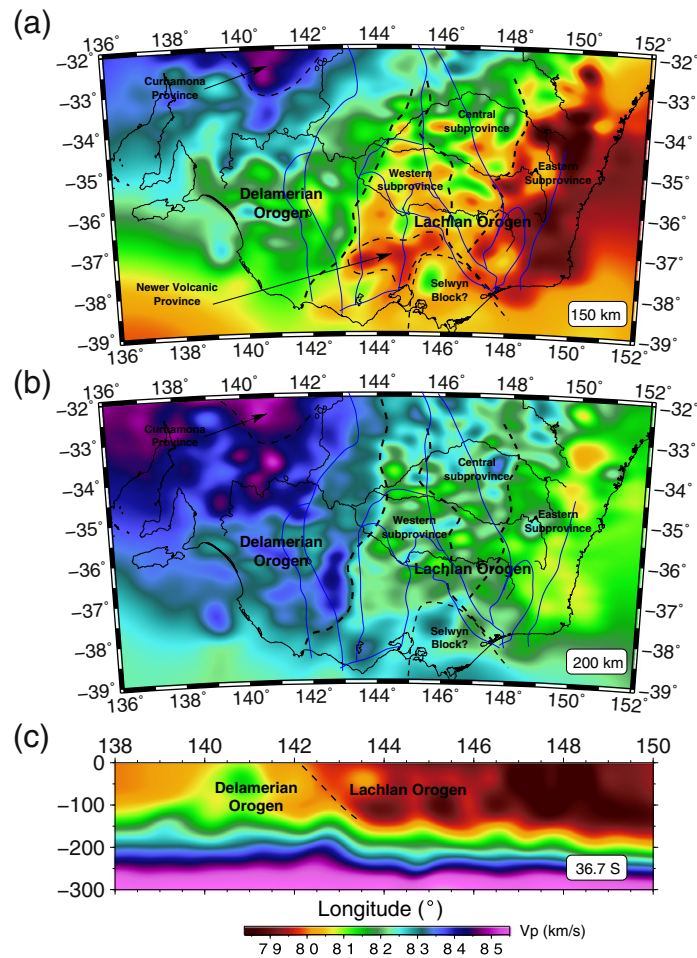


Fig. 11. A selection of slices through the surface wave and body wave solution model with a number of features highlighted. Blue lines indicate the location of observed and inferred terrane boundaries at the surface. (a) Slice at 150 km depth; (b) slice at 200 km depth; and (c) E-W section at 36.7° south. (For interpretation of the references to colour in this figure legend, the reader is referred to the web version of this article.)

Australia, and the presence of the Newer Volcanic Province. Basaltic underplating beneath the crust, caused by lithospheric detachment faults that produce asymmetric margins (Lister et al., 1986) may also have occurred, thus further complicating an already difficult interpretation.

With regard to the Lachlan–Delamerian boundary, one of the more critical considerations is the presence of the Newer Volcanic Provinces north and west of Melbourne. This volcanic centre, which last erupted in the Quaternary, is clearly associated with low velocities at depth (e.g. Fig. 8, Fig. 11a), which can be directly related to the elevated temperatures associated with a magmatic plumbing system. At 100 km depth the NVP appears to be part of a broader low velocity region, which, in models from surface waves alone, has centred on Bass Strait (e.g. Fishwick et al., 2008). However, at 150 km depth, the combination of body wave tomography clearly reveals a distinct low velocity anomaly focused on a much narrower region beneath the NVP. The contrast in lateral extent of the velocity anomaly at these depths may relate to the propensity of plumes to broaden on contact with the lithosphere (e.g. Moore et al., 1998). However, the disappearance of the low velocity anomaly by depths of 200 km certainly raises the alternative possibility that the magmatics are not linked to plume-like upwellings but instead can be associated with alternative processes such as edge driven convection (e.g. Demidjuk et al., 2007; Farrington et al., 2010). It is likely that these anomalies related to the NVP have obfuscated the Delamerian–Lachlan boundary in southern Victoria to some extent. However, the fact that the NVP is no longer visible at 200 km depth, and that the general trend of the Delamerian–Lachlan boundary from NSW

into Victoria is relatively continuous, suggests that the seismic signature of the Delamerian–Lachlan boundary can still be observed through much of the region.

In terms of delineating the subprovinces of the Lachlan Orogen at mantle depths, the combined surface and body wave model produces mixed results. A significant easterly drop in velocity between what has been labelled the Central and Eastern subprovinces (Fig. 11) may represent the deep boundary between the two terranes, but it should also be acknowledged that elevated temperatures due to lithospheric thinning may also be a factor. There is certainly no clear boundary between the Central and Western subprovinces, although on average it could be argued that the Central Subprovince exhibits higher average velocities than either of the two neighbouring terranes, particularly at depths of around 150 km. The Central Subprovince largely incorporates the Omeo Zone (Fig. 1), which represents a band of Palaeozoic intermediate-to-high grade, low pressure metamorphism (Foster and Gray, 2000), possibly formed by eastward subduction beneath an island-arc complex followed by double-divergent subduction (Foster and Gray, 2000; Spaggiari et al., 2003). When relative arrival time residuals from WOMBAT are inverted in the presence of a simple radial model (Rawlinson et al., 2011), the Central Subprovince stands out more clearly as a positive velocity anomaly. The fact that it is less clear in this study is a reflection of the influence that the surface wave model has on the final result.

In the last few years, the argument for the presence of a Proterozoic continental fragment beneath the Melbourne Zone in Victoria (see Fig. 1) – which extends south through Bass Strait to form the Precambrian

fabric of western Tasmania – has been significantly strengthened by recent seismic reflection profiling in the region (Cayley, 2011). Fig. 11a–b does show some evidence for elevated velocities beneath the Melbourne Zone, but the lack of good resolution combined with the more recent overprinting effects of the Newer Volcanic Province have conspired to make reliable interpretation difficult.

6. Conclusions

New results from the WOMBAT transportable seismic array, which combine constraints from teleseismic arrival time residuals and regional surface waves, have illuminated the 3-D seismic structure beneath southeast Australia. An initial P-wave velocity model is constructed from S-wave velocity models – produced by partitioned waveform inversion of the surface waves – assuming $ak135$ Vp/Vs velocity ratios. The minimum scale length of structure constrained by the surface waves is similar to the aperture of the transportable arrays used to record the teleseismic body waves. Consequently, they provide complementary information on long wavelength structural variations that are filtered out by using relative arrival time residuals, which are only sensitive to velocity anomalies with scale lengths smaller than the aperture of the transportable array. Due to these differences in scale, a joint inversion of the two data types would not necessarily yield more information. The success of the hybrid approach used in this study allows new inferences to be made about the structure and tectonic evolution of eastern Australia. In particular: (1) The Palaeo-Proterozoic Curnamona Province is revealed as a velocity high, which not only penetrates to at least 200 km in depth, but also extends southward in the lithospheric mantle some 100 km beyond its surface expression; (2) the Delamerian–Lachlan boundary is imaged as an eastward-dipping transition from higher to lower velocity in the mantle that extends beneath the Western Subprovince of the Lachlan Orogen. The strong velocity contrast observed at 150–200 km depth may be due to differences between the root of the older Delamerian lithosphere and the sublithospheric mantle beneath the younger and thinner lithosphere of the Lachlan Orogen; (3) the Quaternary Newer Volcanic Province is underlain by a distinct low velocity zone to a depth of approximately 150 km, which is likely due to elevated temperatures associated with a hot spot in the uppermost mantle. The absence of low velocities in the deeper mantle favours edge driven convection as a mechanism for hot spot formation, but the presence of a narrow plume feeding the hot spot from the lower mantle cannot be ruled out by this study due to limits on horizontal resolution; (4) an overall decrease in lithospheric velocities in the mantle to the east is thought to reflect a thinning of the lithosphere towards the Australia–Pacific passive margin, although this may be enhanced by the presence of thicker crust beneath the Great Dividing Range.

References

Aki, K., Christoffersson, A., Husebye, E.S., 1977. Determination of the three-dimensional seismic structure of the lithosphere. *Journal of Geophysical Research* 82, 277–296.

Allen, R.M., Nolet, G., Morgan, W.J., Vogfjörð, Bergsson, B.H., Erlendsson, P., Foulger, G.R., Jakobsdóttir, S., Julian, B.R., Pritchard, M., Ragnarsson, S., Stefánsson, R., 2002. Imaging the mantle beneath Iceland using integrated seismological techniques. *Journal of Geophysical Research* 107. doi:10.1029/2001JB000595.

Antolik, M., Gu, Y.J., Ekstrom, G., Dziewonski, A.M., 2003. A new joint model of compressional and shear velocity in the Earth's mantle. *Geophysical Journal International* 153, 443–466.

Arroucau, P., Rawlinson, N., Sambridge, M., 2010. New insight into Cainozoic sedimentary basins and Palaeozoic suture zones in southeast Australia from ambient noise surface wave tomography. *Geophysical Research Letters* 37, L07303. doi:10.1029/2009GL0141974.

Baillie, P.W., 1985. A Palaeozoic suture in eastern Gondwanaland. *Tectonics* 4, 653–660.

Benz, H.M., Zandt, G., Oppenheimer, D.H., 1992. Lithospheric structure of northern California from teleseismic images of the upper mantle. *Journal of Geophysical Research* 97, 4791–4807.

Betts, P.G., Giles, D., Lister, G.S., Frick, L., 2002. Evolution of the Australian lithosphere. *Australian Journal of Earth Sciences* 49, 661–695.

Burdick, S., Li, C., Martynov, V., Cox, T., Eakins, J., Astiz, L., Vernon, F.L., Pavlis, G.L., Van der Hilst, R.D., 2008. Upper mantle heterogeneity beneath North America from travel time tomography with global and USArray transportable array data. *Seismological Research Letters* 79, 384–392.

Cammarano, F., Goes, S., Vacher, P., Giardini, D., 2003. Inferring upper-mantle temperatures from seismic velocities. *Physics of the Earth and Planetary Interiors* 138, 197–222.

Cayley, R., 2011. Exotic crustal block accretion to the eastern Gondwana margin in the Late Cambrian–Tasmania, the Selwyn Block, and implications for the Cambrian–Silurian evolution of the Ross, Delamerian and Lachlan orogens. *Gondwana Research* 19, 628–649.

Cayley, R., Taylor, D.H., VandenBerg, A.H.M., Moore, D.H., 2002. Proterozoic–Early Palaeozoic rocks and the Tyennan Orogeny in central Victoria: the Selwyn Block and its tectonic implications. *Australian Journal of Earth Sciences* 49, 225–254.

Chevrot, S., 2002. Optimal measurements of relative and absolute delay times by simulated annealing. *Geophysical Journal International* 151, 164–171.

Clifford, P., Greenhalgh, S., Houseman, G., Graeber, F., 2008. 3-d seismic tomography of the Adelaide fold belt. *Geophysical Journal International* 172, 167–186.

Conor, C.H.H., Preiss, W.V., 2008. Understanding the 1720–1640 Ma Palaeoproterozoic Willyama Supergroup, Curnamona Province, Southeastern Australia: implications for tectonics, basin evolution and ore genesis. *Precambrian Research* 166, 297–317.

Crawford, A.J., Berry, R.F., 1992. Tectonic implications of Late Proterozoic–Early Palaeozoic igneous rock associations in western Tasmania. *Tectonophysics* 214, 37–56.

Crawford, A.J., Meffre, S., Symonds, P.A., 2003. 120 to 0 Ma tectonic evolution of the southwest Pacific and analogous geological evolution of the 600 to 220 Ma Tasman Fold Belt System. *Geological Society of Australia Special Publication and Geological Society of America Special Publication*, pp. 383–404.

Debayle, E., Kennett, B.L.N., 2000. The Australian continental upper mantle: structure and deformation inferred from surface waves. *Journal of Geophysical Research* 105, 25,423–25,450.

Demidjuk, Z., Turner, S., Sandiford, M., Rhiannon, G., Foden, J., Etheridge, M., 2007. U-series isotope and geodynamic constraints on mantle melting processes beneath the newer volcanic province in South Australia. *Earth and Planetary Science Letters* 261, 517–533.

Direen, N.G., Crawford, A.J., 2003a. Fossil seaward-dipping reflector sequences preserved in southeastern Australia: a 600 Ma volcanic passive margin in eastern Gondwanaland. *Journal of the Geological Society* 160, 985–990.

Direen, N.G., Crawford, A.J., 2003b. The Tasman Line: where is it, what is it, and is it Australia's Rodinian breakup boundary? *Australian Journal of Earth Sciences* 50, 491–502.

Farrington, R.J., Stegman, D.R., Moresi, L.N., Sandiford, M., May, D.A., 2010. Interactions of 3d mantle flow and continental lithosphere near passive margins. *Tectonophysics* 483, 20–28.

Faul, U.H., Jackson, I., 2005. The seismological signature of temperature and grain size variations in the upper mantle. *Earth and Planetary Science Letters* 234, 119–134.

Fichtner, A., Kennett, B.L.N., Igel, H., Bunge, H.-P., 2009. Full waveform tomography for upper-mantle structure in the Australasian region using adjoint methods. *Geophysical Journal International* 179, 1703–1725.

Fishwick, S., Heintz, M., Kennett, B.L.N., Reading, A.M., Yoshizawa, K., 2008. Steps in lithospheric thickness within eastern Australia, evidence from surface wave tomography. *Tectonics* 27. doi:10.1029/2007TC002116.

Fishwick, S., Kennett, B.L.N., Reading, A.M., 2005. Contrasts in lithospheric structure within the Australian craton – insights from surface wave tomography. *Earth and Planetary Science Letters* 231, 163–176.

Foden, J., Elburg, M.A., Dougherty-Page, J., Burt, A., 2006. The timing and duration of the Delamerian Orogeny: correlation with the Ross Orogen and implications for Gondwana assembly. *Journal of Geology* 114, 189–210.

Foster, D.A., Gleadow, A.J.W., 1992. Reactivated tectonic boundaries and implications for the reconstruction of south-eastern Australia and Northern Victoria land. *Antarctica Geology* 20, 267–270.

Foster, D.A., Gray, D.R., 2000. Evolution and structure of the Lachlan Fold Belt (Orogen) of eastern Australia. *Annual Review of Earth and Planetary Sciences* 28, 47–80.

Frederiksen, A.W., Bostock, M.G., VanDecar, J.C., Cassidy, J.F., 1998. Seismic structure of the upper mantle beneath the northern Canadian Cordillera from teleseismic travel-time inversion. *Tectonophysics* 294, 43–55.

Gaina, C., Müller, D., Royer, J.-Y., Stock, J., Hardebeck, J., Symonds, P., 1998. The tectonic history of the Tasman Sea: a puzzle with 13 pieces. *Journal of Geophysical Research* 103, 12,413–12,433.

Gibson, G.M., Morse, M.P., Ireland, T.R., Nayak, G.K., 2011. Arc-continent collision and orogenesis in western tasmanides: insights from reactivated basement structures and formation of an ocean-continent transform boundary off western Tasmania. *Gondwana Research* 19, 608–627.

Glahn, A., Granet, M., 1993. Southern Rhine Graben: small-wavelength tomographic study and implications for the dynamic evolution of the graben. *Geophysical Journal International* 113, 399–418.

Glen, R.A., 2005. The Tasmanides of eastern Australia. In: Vaughan, A.P.M., Leat, P.T., Pankhurst, R.J. (Eds.), *Terrane Processes at the Margins of Gondwana*. Geological Society, London, pp. 23–96.

Glen, R.A., Percival, I.G., Quinn, C.D., 2009. Ordovician continental margin terranes in the Lachlan Orogen, Australia: implications for tectonics in an accretionary orogen along the east Gondwana margin. *Tectonics* 28. doi:10.1029/2009TC002446.

Graeber, F.M., Asch, G., 1999. Three-dimensional models of P wave velocity and P-to-S velocity ratio in the southern central Andes by simultaneous inversion of local earthquake data. *Journal of Geophysical Research* 104, 20,237–20,256.

Graeber, F.M., Houseman, G.A., Greenhalgh, S.A., 2002. Regional teleseismic tomography of the western Lachlan Orogen and the Newer Volcanic Province, southeast Australia. *Geophysical Journal International* 149, 249–266.

- Griffin, W.L., O'Reilly, S.Y., Ryan, C.G., Gaul, O., Ionov, D.A., 1998. Secular variation in the composition of subcontinental lithospheric mantle: geophysical and geodynamic implications. In: Braun, J., Dooley, J., Goleby, B., van der Hilst, R., Klotwijk, C. (Eds.), *Structure and Evolution of the Australian Continent: American Geophysical Union Geodynamic Series*, Vol. 26, pp. 1–26.
- Gunn, P.J., Mitchell, J., Meixner, A., 1997. The structure and evolution of the bass basin as delineated by aeromagnetic data. *Exploration Geophysics* 28, 214–219.
- Hearn, T.M., Clayton, R.W., 1986. Lateral velocity variations in southern California. I. Results for the upper crust from *Pg* waves. *Bulletin Seismological Society of America* 76, 495–509.
- Kemp, A.I.S., Hawkesworth, C.J., Collins, W.J., Gray, C.M., Blevin, P.L., EIMF, 2009. Isotopic evidence for rapid continental growth in an extensional accretionary orogen: the Tasmanides, eastern Australia. *Earth and Planetary Science Letters* 284, 455–466.
- Kennett, B.L.N., 2003. Seismic structure in the mantle beneath Australia. In: Hillis, R.R., Müller, R.D. (Eds.), *Evolution and Dynamics of the Australian Plate*. : Special Publication, Vol. 22. Geological Society of Australia, pp. 7–23.
- Kennett, B.L.N., Engdahl, E.R., Buland, R., 1995. Constraints on seismic velocities in the earth from travel times. *Geophysical Journal International* 122, 108–124.
- Kennett, B.L.N., Sambridge, M.S., Williamson, P.R., 1988. Subspace methods for large scale inverse problems involving multiple parameter classes. *Geophysical Journal* 94, 237–247.
- Knight, L.A., McDonald, P.A., Frankel, E., Moore, D.H., 1995. A preliminary appraisal of the pre-Tertiary intrabasins beneath the Murray Basin, northwestern Victoria. Department of Agriculture, Energy and Minerals, Victorian Initiative for Minerals and Petroleum Report.
- Korsch, R.J., Barton, T.J., Gray, D.R., Owen, A.J., Foster, D.A., 2002. Geological interpretation of a deep seismic-reflection transect across the boundary between the Delamerian and Lachlan Orogens, in the vicinity of the Grampians, western Victoria. *Australian Journal of Earth Sciences* 49, 1057–1075.
- Leaman, D.E., 1994. The Tamar fracture system in Tasmania: does it exist? *Australian Journal of Earth Sciences* 41, 73–74.
- Lei, J., Zhao, D., 2007. Teleseismic P-wave tomography and the upper mantle structure of the central Tien Shan orogenic belt. *Physics of the Earth and Planetary Interiors* 162, 165–185.
- Lévéque, J.J., Masson, F., 1999. From ACH tomographic models to absolute velocity models. *Geophysical Journal International* 137, 621–629.
- Lévéque, J.J., Rivera, L., Wittlinger, G., 1993. On the use of the checker-board test to assess the resolution of tomographic inversions. *Geophysical Journal International* 115, 313–318.
- Lister, G.S., Ethridge, M.A., Symonds, P.A., 1986. Detachment faulting and the evolution of passive continental margins. *Geology* 14, 246–250.
- Lister, G.S., Ethridge, M.A., Symonds, P.A., 1991. Detachment models for the formation of passive continental margins. *Tectonics* 10, 1038–1064.
- Martin, M., Ritter, J.R.R., the CALIXTO working group, 2005. High-resolution teleseismic body-wave tomography beneath SE Romania – I. Implications for the three-dimensional versus one-dimensional crustal correction strategies with a new crustal velocity model. *Geophysical Journal International* 162, 448–460.
- Mégnin, C., Romanowicz, B., 2000. The three-dimensional shear velocity structure of the mantle from the inversion of body, surface and higher-mode waveforms. *Geophysical Journal International* 143, 709–728.
- Moore, W.B., Schubert, G., Tackley, P., 1998. Three-dimensional simulations of plume-lithosphere interaction at the Hawaiian Swell. *Science* 279, 1008–1011.
- Obrebski, M., Allen, R.M., Pollitz, F., Hung, S.-H., 2011. Lithosphereasthenosphere interaction beneath the western United States from the joint inversion of body-wave traveltimes and surface-wave phase velocities. *Geophysical Journal International* 185, 1003–1021.
- Oncescu, M.C., Burlacu, V., Anghel, M., Smalbergher, V., 1984. Three-dimensional *P*-wave velocity image under the Carpathian Arc. *Tectonophysics* 106, 305–319.
- Powell, C.M., Baillie, P.W., 1992. Tectonic affinity of the Mathina Group in the Lachlan Fold Belt. *Tectonophysics* 214, 193–209.
- Price, R.C., Gray, C.M., Frey, F.A., 1997. Strontium isotopic and trace element heterogeneity in the plains basalts of the Newer Volcanic Province, Victoria, Australia. *Geochimica et Cosmochimica Acta* 61, 171–192.
- Rawlinson, N., Kennett, B., Vanacore, E., Glen, R., Fishwick, S., 2011. The structure of the upper mantle beneath the Delamerian and Lachlan orogens from simultaneous inversion of multiple teleseismic datasets. *Gondwana Research* 19, 788–799.
- Rawlinson, N., Kennett, B.L.N., 2004. Rapid estimation of relative and absolute delay times across a network by adaptive stacking. *Geophysical Journal International* 157, 332–340.
- Rawlinson, N., Kennett, B.L.N., 2008. Teleseismic tomography of the upper mantle beneath the southern Lachlan Orogen, Australia. *Physics of the Earth and Planetary Interiors* 167, 84–97.
- Rawlinson, N., Kennett, B.L.N., Heintz, M., 2006a. Insights into the structure of the upper mantle beneath the Murray Basin from 3D teleseismic tomography. *Australian Journal of Earth Sciences* 53, 595–604.
- Rawlinson, N., Pozgay, S., Fishwick, S., 2010a. Seismic tomography: a window into deep Earth. *Physics of the Earth and Planetary Interiors* 178, 101–135.
- Rawlinson, N., Reading, A.M., Kennett, B.L.N., 2006b. Lithospheric structure of Tasmania from a novel form of teleseismic tomography. *Journal of Geophysical Research* 111. doi:10.1029/2005JB003803.
- Rawlinson, N., Sambridge, M., 2004. Wavefront evolution in strongly heterogeneous layered media using the fast marching method. *Geophysical Journal International* 156, 631–647.
- Rawlinson, N., Tkalčić, H., Reading, A.M., 2010b. Structure of the Tasmanian lithosphere from 3-D seismic tomography. *Australian Journal of Earth Sciences* 57, 381–394.
- Rawlinson, N., Urvoy, M., 2006. Simultaneous inversion of active and passive source datasets for 3-D seismic structure with application to Tasmania. *Geophysical Research Letters* 33. doi:10.1029/2006GL028105.
- Reed, A.R., Calver, C., Bottrill, R.S., 2002. Palaeozoic suturing of eastern and western Tasmania in the west Tamar region: implications for the tectonic evolution of southeast Australia. *Australian Journal of Earth Sciences* 49, 809–830.
- Roth, J.B., Fouch, M.J., James, D.E., Carlson, R.W., 2008. Three-dimensional seismic velocity structure of the northwestern United States. *Geophysical Research Letters* 35, L15304. doi:10.1029/2008GL034669.
- Saltzer, R.L., Humphreys, E.D., 1997. Upper mantle *P* wave velocity structure of the eastern Snake River Plain and its relationship to geodynamic models of the region. *Journal of Geophysical Research* 102, 11,829–11,841.
- Simons, F., Zielhuis, A., van der Hilst, R.D., 1999. The deep structure of the Australian continent from surface wave tomography. *Lithos* 48, 17–43.
- Simons, F.J., van der Hilst, R.D., Montagner, J.-P., Zielhuis, A., 2002. Multimode Rayleigh wave inversion for heterogeneity and azimuthal anisotropy of the Australian upper mantle. *Geophysical Journal International* 151, 738–754.
- Spaggiari, C.V., Gray, D.R., Foster, D.A., 2004. Lachlan Orogen subduction-accretion systematics revisited. *Australian Journal of Earth Sciences* 51, 549–553.
- Spaggiari, C.V., Gray, D.R., Foster, D.A., McKnight, S., 2003. Evolution of the boundary between the western and central Lachlan Orogen: implications for Tasmanide tectonics. *Australian Journal of Earth Sciences* 50, 725–749.
- Talent, J.A., Banks, M.R., 1967. Devonian of victoria and tasmania. In: Oswald, D.H. (Ed.), *International Symposium on the Devonian System: Alberta Soc. Pet. Geol., Alberta*, pp. 147–163.
- Taylor, D.H., Cayley, R.A., 2000. Character and kinematics of faults within the turbidite-dominated Lachlan Orogen: implications for tectonic evolution of eastern Australia: discussion. *Journal of Structural Geology* 22, 523–528.
- Tkalčić, H., Rawlinson, N., Arroucau, P., Kumar, A., Kennett, B. L. N., 2011. Multi-Step modeling of receiver-based seismic and ambient noise data from WOMBAT array: Crustal structure beneath southeast Australia. *J. Geophys. Res.* Submitted.
- VanDecar, J.C., Crosson, R.S., 1990. Determination of teleseismic relative phase arrival times using multi-channel cross-correlation and least squares. *Bulletin Seismological Society of America* 80, 150–169.
- VandenBerg, A.H.M., 1978. The Tasman fold belt system in Victoria. *Tectonophysics* 48, 267–297.
- VandenBerg, A.H.M., 1999. Timing of orogenic events in the Lachlan Orogen. *Australian Journal of Earth Sciences* 46, 691–701.
- Waldhauser, F., Lippitsch, R., Kissling, E., Anson, J., 2002. High-resolution teleseismic tomography of upper-mantle structure using an *a priori* three-dimensional crustal model. *Geophysical Journal International* 150, 403–414.
- Webster, A.E., 1996. Delamerian refolding of the Palaeoproterozoic Broken Hill Block. *Australian Journal of Earth Sciences* 43, 85–89.
- West, M., Gao, W., Grand, S., 2004. A simple approach to the joint inversion of seismic body and surface waves applied to the southwest U.S. *Geophysical Research Letters* 31.
- Willman, C.E., VandenBerg, A.H.M., Morand, V.J., 2002. Evolution of the southeastern Lachlan Fold Belt in Victoria. *Australian Journal of Earth Sciences* 49, 271–289.
- Yoshizawa, K., Kennett, B.L.N., 2004. Multimode surface wave tomography for the Australian region using a three-stage approach incorporating finite frequency effects. *Journal of Geophysical Research* 109. doi:10.1029/2002JB002254.
- Zielhuis, A., van der Hilst, R.D., 1996. Upper-mantle shear velocity beneath eastern Australia from inversion of waveforms from SKIPPY portable arrays. *Geophysical Journal International* 127, 1–16.